

**NOAA NESDIS
CENTER FOR SATELLITE APPLICATIONS
AND RESEARCH
GEOSTATIONARY & POLAR BLENDED
SEA SURFACE TEMPERATURE
ANALYSIS
(GEO-POLAR BLENDED SST)
ALGORITHM THEORETICAL BASIS
DOCUMENT
Version 2.1**

NOAA NESDIS STAR

ALGORITHM THEORETICAL BASIS DOCUMENT

Version: 2.0

Date: May 15, 2012

TITLE: Geo-Polar Blended SST Algorithm Theoretical Basis Document

Page 2 of 44

TITLE: GEO-POLAR BLENDED SST ALGORITHM THEORETICAL BASIS DOCUMENT
VERSION 2.1

AUTHORS:

Andrew Harris (NOAA/NESDIS/CICS, UMD)

Eileen Maturi (NOAA/NESDIS/STAR)

GOES LST ALGORITHM THEORETICAL BASIS DOCUMENT
VERSION HISTORY SUMMARY

Version	Description	Revised Sections	Date
1.0	New document adapted from STAR EPL guidelines	New Document	4/26/2012
2.0	Updated Document	References	5/15/2012
2.1	Updated Document	References	3/21/2013

TABLE OF CONTENTS

	<u>Page</u>
LIST OF FIGURES.....	5
LIST OF TABLES.....	6
LIST OF ACRONYMS.....	7
ABSTRACT.....	8
1. INTRODUCTION.....	9
1.1. Purpose of This Document.....	9
1.2. Who Should Use This Document.....	9
1.3. Inside Each Section.....	9
1.4. Revision History.....	10
2. SYSTEM OVERVIEW.....	11
2.1 Products Generated.....	11
2.2 Instrument Characteristics.....	12
2.3 Product Requirement.....	13
2.4 Retrieval Strategies.....	14
3. ALGORITHM DESCRIPTION.....	15
3.1 Processing Overview.....	15
3.2 Algorithm Input.....	16
3.2.1 Derived Sensor Data.....	17
3.2.2 Ancillary Data.....	18
3.2.3 Static and internal analysis/observation state values.....	18
3.3 Theoretical Description.....	19
3.3.1 Physical Description.....	19
3.3.2 Mathematical Description.....	21
3.3.3 Summary of Algorithm Selection.....	26
3.4 Algorithm Output.....	27
3.5 Performance Estimates.....	28

NOAA NESDIS STAR

ALGORITHM THEORETICAL BASIS DOCUMENT

Version: 2.0

Date: May 15, 2012

TITLE: Geo-Polar Blended SST Algorithm Theoretical Basis Document

Page 4 of 44

3.5.1 Test Data	28
3.5.1.1 Geostationary SST Data	28
3.5.1.2 Polar-orbiting SST Data	29
3.5.1.3 Ground truth data	29
3.5.1.4 Match-ups	29
3.5.2 Results	30
3.5.2.1 Precision and Accuracy Estimates	31
3.5.2.2 Error Budget	33
3.6 Practical Considerations	35
3.6.1 Numerical Computation Considerations	35
3.6.2 Programming and Procedural Considerations	36
3.6.2.1 Configuration of Analysis	36
3.6.3 Quality Assessment and Diagnostics	37
3.6.4 Exception Handling	37
3.7 Validation	38
4. ASSUMPTIONS AND LIMITATIONS	39
4.1 Assumptions	39
4.2 Limitations	39
4.3 Potential Improvements	39
4.3.1 Improved Validation Methods	39
4.3.2 Algorithm Improvements	40
5. LIST OF REFERENCES	42

LIST OF FIGURES

	<u>Page</u>
Figure 3.1 Standard prediction-update process	21
Figure 3.2 Simple multi-scale tree	25
Figure 3.3 Location of in situ data from iQuam database	28
Figure 3.4 Validation of 5-km Geo-Polar Blended SST	30
Figure 3.5 One day's worth of geostationary and polar-orbiting SST data	32
Figure 3.6 Daytime bias correction for GOES-E and NOAA AVHRR SST products	32
Figure 3.7 Relationship between full domain and individual tiles	35

LIST OF TABLES

	<u>Page</u>
Table 2.1. Spectral characters of GOES-12 through -15 Imager	13
Table 3.1. Input list of geostationary (GOES-E/W, MTSAT, MSG) derived sensor data	17
Table 3.2. Input list of ACSPO polar-orbiting (NOAA-19, METOP) derived sensor data	17
Table 3.3 Input of ancillary data	18
Table 3.4. Algorithm output data	27
Table 3.5 Detailed descriptions of the mask byte set at the pixel level	28
Table 3.6. Precision and Accuracy (in kelvin)	32
Table 3.7. Error Budget (in kelvin)	34
Table 3.8. Quad-tree tile parameters	35

NOAA NESDIS STAR

ALGORITHM THEORETICAL BASIS DOCUMENT

Version: 2.0

Date: May 15, 2012

TITLE: Geo-Polar Blended SST Algorithm Theoretical Basis Document

Page 7 of 44

LIST OF ACRONYMS

ACSPO	Advanced Clear Sky Processor for Oceans
AMSR	Advanced Scanning Microwave Radiometer
ATBD	Algorithm Theoretical Base Document
AVHRR	Advanced Very High Resolution Radiometer
CRW	Coral Reef Watch
CW	CoastWatch
ECV	Essential Climate Variable
EDR	Environmental Data Record
EQX	Equator crossing time
ENVISAT	ENVironmental SATellite
EUMETSAT	EUropean organisation for the exploitation of METeorological SATellites
GCOM-W	Global Change Observation Mission-Water
GCOS	Global Climate Observing System
GOES	Geostationary Operational Environmental Satellite
GHRSSST	Group for High Resolution Sea Surface Temperature
HDF	Hierarchical Data Format
IR	Infrared
JMA	Japan Meteorological Agency
METOP	METeorological OPERational satellite
NetCDF	Network Common Data Form
MSG	Meteosat Second Generation
MTSAT-2	Multifunction Transport SATellite - 2
NESDIS	National Environmental Satellite, Data, and Information Service
NCEP	National Centers for Environmental Prediction
NOAA	National Oceanic and Atmospheric Administration
OI	Optimal Interpolation
OPC	Ocean Products Center
QC	Quality Control
SEVIRI	Spinning Enhanced Visible Infra-Red Imager
SWA	Software Architecture Document
TPW	Total Precipitable Water

ABSTRACT

This Algorithm Theoretical Basis Document (ATBD) describes in detail the procedures for developing a global blended SST analysis from NOAA operational satellite SST products. The actual methodology for deriving the level 2 SST products themselves is not in any significant detail. The main part of the ATBD is a description of the science and methodology for combining polar and geostationary SST products into a single daily global analysis at $0.05^\circ \times 0.05^\circ$ resolution. This includes descriptions of the preprocessing steps for data ingest and gridding, quality control and bias correction, as well as the particular aspects of the analysis procedure which make it unique with respect to typical optimal interpolation techniques. The required ancillary data and their roles are also described, and the characteristics of the final product are evaluated.

The input data are all generated on an operational basis "in-house" at NOAA. The geostationary platforms include operational NOAA GOES-E (75°W) and GOES-W (135°W), and also Meteosat-9 (0°E) and MTSAT-2 (145°E), operated by EUMETSAT and JMA respectively. Polar orbiter data are provided by the operational NOAA-19 (EQX $\sim 14:00$ local time) and METOP-A (EQX $\sim 10:30$ local time) satellites, operated by NOAA and EUMETSAT respectively.

Input data are bias corrected with reference to the operational NCEP RTG_HR SST Analysis product. This is found to be an essential step prior to operation of the analysis estimator.

1. INTRODUCTION

The purpose, users, scope, related documents and revision history of this document are briefly described in this section. Section 2 gives an overview of the SST analysis objectives and operations concept. Section 3 describes the baseline algorithm, its input data requirements, the theoretical background, required preprocessing steps and error budgeting. Test data sets and outputs are presented in Section 4. Some practical considerations are described in Section 5, followed by the assumptions and limitations associated with the algorithm in Section 6. Finally, Section 7 lists the references cited.

1.1. Purpose of This Document

This Algorithm Theoretical Basis Document (ATBD) explains the physical and mathematical background for an algorithm to derive a 5-km resolution daily global SST analysis product from NOAA's operationally produced satellite SST products. This document provides an overview of the required input data, the physical and mathematical backgrounds of the described algorithm, practical considerations, and assumptions and limitations.

1.2. Who Should Use This Document

The intended users of this document are those interested in understanding the mathematical and practical computational aspects of the analysis and how the analysis performs for the current input data. This document also provides information useful to anyone maintaining or modifying the original algorithm.

1.3. Inside Each Section

This ATBD includes four sections:

Section 1.0 – Introduction. provides the purpose, intended users, and revision history of the ATBD.

Section 2.0 – System Overview, describes the products generated by the algorithm and the characteristics of the level 2 products that supply inputs to the algorithm.

Section 3.0 - Algorithm Description, provides the algorithm details including a processing overview, input data, physical description, mathematical description, algorithm output, performance estimates, practical considerations, and validation.

Section 4.0 – Assumptions and Limitations, states assumptions presumed in determining that the software system architecture as designed will meet the requirements, and states limitations that may impact on the system’s ability to meet requirements.

Section 5.0 - List of References, gives a list of references cited in the document.

1.4. Revision History

This is the first version (1.0) of the Geo-Polar Blended SST ATBD produced for the operational launch of the 5-km (0.05 degree) version of the analysis. There was a previous version for the 11-km (0.1 degree) analysis which did not conform to the STAR template. Furthermore, the previous version had functionally more in common with a Users’ Guide than an ATBD.

2. SYSTEM OVERVIEW

This section describes objectives of the Geo-Polar Blended SST Analysis algorithm, characteristics of the geostationary and polar SST products, and the product requirements.

2.1 Products Generated

Sea surface temperature, a GCOS Essential Climate Variable and key EDR, is widely required in applications of hydrology, meteorology, oceanography and climatology. It is of fundamental importance to the storage and transport of heat within the ocean-atmosphere system. Temperatures at the Earth's surface are important for the study of climate change, and, due to the large heat capacity of the ocean (the top 3 meters contain as much heat as the entire atmosphere), SST is the most reliable and stable of possible temperature measurements. Satellite SSTs are also be assimilated into climate, mesoscale atmospheric and oceanic models to estimate sensible and latent heat fluxes. They can also be applied for analyzing climate change due to its rich archive from being routinely produced from imagery data of geostationary and polar-orbiting satellites.

NOAA routinely generates SST products from data provided by polar-orbiting (AVHRR, carried on-board NOAA and METOP platforms) and geostationary thermal infrared sensors (Imagers carried on board GOES-E/W and MTSAT-2 platforms, and the SEVIRI carried on board MSG) (*Maturi, et al, 2008*). Due to the nature of the infrared observations, only cloud-free areas may return a valid SST, thus each derived Level-2 product will have gaps where the cloud detection process has identified cloud contamination. While this is not an issue for certain applications, many users desire a gridded gap-free "best estimate" of the SST for a given day. The importance of such products can be ascertained by the fact that the reference paper for NOAA's well-known 1-degree OI SST product (Reynolds & Smith, 1994) has over two thousand citations.

While a 1-degree resolution SST analysis has value in certain applications, there has been a recent push towards generating analyses of much higher resolution. NESDIS now produce a "1/4° Daily-OI" product, while NCEP's latest SST analysis has a nominal grid resolution of 1/12°. Other institutes routinely produce analyses at 0.1° or 0.05° grid resolution, and there are even some global analyses that approach the 1-km scale. As will be seen later, grid resolution does not always equate to resolving power.

The reason for proliferation for these high resolution products is that there are new applications which demand them. Mesoscale and coastal oceanography require the ability to resolve at the [latitude-dependent] Rossby radius, which requires sampling at half the wavelength. The main problem is that, unless cloud-free observations exist, results must

be obtained by interpolation. Such interpolation is usually performed by obtaining a weighted average over a certain search radius, and the size of the radius determines the effective analysis resolution. If high resolution is required then the radius must be short, which leads to the risk of having very few observations contributing to the estimate, with a concomitant impact on product noise. This is a problem which all OI-type analyses face.

While little can be done in persistently cloudy regions, the use of geostationary SST products permits the recovery of relatively complete observation field over a 24-hour period. However, geostationary SST products are generally considered less accurate than those obtained from polar-orbiting instruments, and many Level-4 data providers eschew their inclusion for fear of degrading the resulting analysis. Here, STAR is at an advantage, since we are responsible for both Level-2 and Level-4 data production, and have intimate knowledge of the geostationary product characteristics.

The first generation of this analysis was produced at 0.1° resolution and was deemed successful in resolving mesoscale oceanographic features – a feat which most other high-resolution SST analyses failed to achieve. The analysis methodology that underpins both the 0.1° analysis and this new 0.05° version is essentially the same. However, in adapting the previous version to run at the new resolution, various aspects of the methodology had to be well-understood in order to optimize the processing.

Applications which have specifically requested the new analysis include the NOAA Coral Reef Watch (CRW) Program and NOAA CoastWatch Program. Others which will make use of it include the NCEP OPC High Seas Forecast, the NHC Ocean Heat Content product, NASA Aquarius Salinity Mission and GHRSSST. Additionally, CRW have requested a nighttime-only product to be more directly comparable with their previous baseline analysis.

2.2 Level 2 Product Characteristics

The Geostationary Operational Environmental Satellite (GOES) system, operated by the United States National Environmental Satellite, Data, and Information Service (NESDIS), supports weather forecasting, severe storm tracking, and meteorology research. The spacecraft sends data to the ground system to provide a continuous stream of environmental data. The National Weather Service (NWS) uses the GOES system for its United States operational weather forecasting and monitoring, and scientific researchers use the data to better understand land, atmosphere, ocean, and climate.

The GOES system uses geosynchronous satellites which—since the launch in 1974—have been a basic element of U.S. weather monitoring and forecasting. Designed to operate in geostationary orbit, 35,790 km (22,240 statute miles) above the earth, thereby remaining

NOAA NESDIS STAR

ALGORITHM THEORETICAL BASIS DOCUMENT

Version: 2.0

Date: May 15, 2012

TITLE: Geo-Polar Blended SST Algorithm Theoretical Basis Document

Page 13 of 44

stationary with respect to a point on the ground, the advanced GOES I–M spacecraft continuously view the continental United States, observing environments of the Pacific and Atlantic Oceans, and Central, South America and southern Canada. Since 1994, a three-axis, body-stabilized spacecraft design enables the sensors to "stare" at the earth and thus obtain better signal-to-noise which benefits imaging clouds, monitoring earth's surface temperature and water vapor fields, and sounding the atmosphere for its vertical thermal and vapor structures.

Table 2.1. Spectral characters of GOES-12 through -15 Imager

Channels	Central Wavelength (μm)	Resolution (km)
1 (visible)	0.65	1 km x 1km
2 (infrared)	3.9	4 km x 4km
3 (infrared)	6.48	4 km x 4km
4 (infrared)	10.7	4 km x 4km
6 (infrared)	13.3	4 km x 8 km (GOES-12/13) 4 km x 4km (GOES-14/15)

Shaded channels are used for the operational GOES SST retrieval. The 13.3 micron channel will be used in the new physical retrieval scheme.

SST product accuracies for the various geostationary sensors can be found on the STAR website:

GOES: http://www.star.nesdis.noaa.gov/sod/meceb/goes_validation/test/index.php

MTSAT: http://www.star.nesdis.noaa.gov/sod/meceb/mtsats_validation/index.php

MSG: http://www.star.nesdis.noaa.gov/sod/meceb/msg_validation/index.php

Product accuracies vary between 0.5 – 1 K depending on sensor and time of observation.

2.3 Product Requirement

The product is to be produced once per day on a global grid of $0.05^\circ \times 0.05^\circ$ resolution. The target accuracy for the product is an accuracy of ± 0.3 K. It is understood that the effective

product resolution and accuracy will vary depending on the availability and accuracy of input data (*i.e.* satellite SST products).

2.4 Analysis Strategies

Viable strategies for obtaining a gap-free product include straightforward OI analysis, assimilation into ocean models of varying complexity, and advanced signal processing techniques such as wavelet analysis. However, while the latter two may offer certain advantages, they are not as mature as OI analysis and require orders of magnitude more computer resources.

Irrespective of the methodology that is selected, a critical first step is the quality control, gridding and bias removal for each of the input datasets. Since virtually all methodologies estimate an innovation from a first guess (usually the previous day's analysis) for each grid point, it is critical that the observed anomalies are as bias and noise free as possible prior to the analysis step. Quality control can be obtained by comparing the difference between the observation and the first guess with the expected ocean variability for that location and the likely noise characteristics of the observation itself. Data which lie more than a given distance outside the combined "noise" threshold may be rejected as "bad". Typically, such departures are colder than the first guess due to cloud contamination but, in the case of GOES daytime SST retrievals, residual cloud contamination may result in an unduly "warm" retrieval since the Imager's 3.9 micron channel is sensitive to solar wavelengths.

It should be noted that all of the Level-2 SST products currently used in the analysis use linear regression methodologies to obtain the SST retrieval. One consequence of this is that variation in atmospheric conditions may produce regional biases. Since these are on the atmospheric spatial scale (of order 1 – 10 degrees), smoothed "observation – analysis" estimates can be used to mitigate such effects. It should also be noted that geostationary data are impacted somewhat differently than polar SST products by such phenomena, since the formers' viewing geometries are fixed with respect to large-scale atmospheric features (sub-tropical high-pressure, *etc.*).

3. ALGORITHM DESCRIPTION

3.1 Processing Overview

The processing outline of the Geo-Polar Blended SST algorithm is as follows.

Major processing steps:

- 1) Average each input data type (e.g. GOES-E daytime or NOAA-19 nighttime) onto analysis grid
 - a. Each input data type is kept as a discrete input by the analysis scheme, e.g. GOES-E daytime and nighttime are not combined in the gridding process
 - b. Data are quality-controlled during the gridding with reference to the previous day's analysis*
 - i. Previous day's bias correction is applied and individual observations are rejected if the deviation from the previous analysis is beyond a certain threshold determined by the anticipated data quality for the observation type, combined with the recent history of SST variability for that location
 - ii. A second internal consistency metric is applied to all data that pass stage (i), if there are sufficient observations (at least 5) within an input grid cell
 - c. NCEP operational ice mask is read onto analysis grid and used to exclude potentially ice-contaminated data
 - i. 0.05° gridded RTG_HR is obtained by bilinear interpolation and saved
 - ii. "Thinned" RTG_HR data (every 3rd pixel and line, i.e. ~1/4°) is used as input to the analysis
 - d. NCEP RTG_HR data are also read in onto analysis grid without QC or bias correction
 - e. Uncertainty estimate is obtained for each grid cell, either by statistics (if there are sufficient input pixels that pass QC), or assigned a default value for each observation type
 - f. Gridded input data are saved in separate Matlab files
- 2) Apply bias correction to each data type
 - a. This is obtained from the previous day's processing (see below)
- 3) Perform multi-scale OI analysis
 - a. Recursive estimator applied to quad-tree 'tiles' of size 128×128
 - b. Analysis is performed at three correlation length scales (8, 16 & 32 grid cells)
 - c. Each designated ocean basin is treated independently, e.g. data in the Atlantic are ignored when calculating the analysis estimate of SST for the Mediterranean
 - d. Final analysis is obtained by interpolating result for each correlation length
 - i. This mimics a non-stationary prior but without the concomitant ambiguity in OI-estimate
 - ii. Interpolation is based on local data density: more data → shorter correlation length
 - e. Tile overlap regions are smoothed to obtain final analysis
- 4) Write out analysis results
 - a. Output product files in various formats (CoastWatch HDF, GHRSSST NetCDF)
 - b. Matlab analysis files (SST analysis, derived correlation length, ocean variability, ice mask, RTG_HR @0.05°)

- 5) Update biases for all satellite input sources
 - a. The gridded input file for each input data type is read in, along with previous day's bias estimate for that data type
 - b. Difference between the satellite SST for each data type and RTG_HR SST is obtained for each grid point
 - c. Bias for each data type is updated by $0.4 \times \text{previous} + 0.6 \times \text{current}$ for each valid grid cell (*i.e.* where data exist for the current day), otherwise left unchanged
 - d. Bias is spatially smoothed over $\pm 1^\circ$ to remove small-scale fluctuations
 - e. Updated bias fields for each data type are saved as a named variable in a Matlab file

*Note that, since the quality control of input data is done with reference to the previous day's SST analysis, the nighttime-only product generation is completely separate, *i.e.* the post-QC input files are different from those used for the day-night analysis product, even for the same data type. *E.g.* GOES-E nighttime gridded input data may be slightly different for the nighttime-only analysis than for the day-night analysis, since the raw satellite data were QC'd against different (night-only *cf.* day-night) analyses.

3.2 Algorithm Input

This section describes the input needed to process the Geo-Polar SST Analysis product. While the SST is derived for each ocean pixel, ancillary datasets are required as well as the upstream geostationary and polar-orbiting Level-2 SST products.

3.2.1 Derived Sensor Data

The geostationary derived sensor data include gridded SST output from the NESDIS Geo-SST processing system (*Maturi, et al, 2008*). While a variety of products are generated, the analysis currently reads in the hourly gridded output files. The polar-orbiting derived sensor data are the ACSPO Table 3.1 briefly describes input of the derived sensor data for the geostationary products.

Table 3.1. Input list of geostationary (GOES-E/W, MTSAT, MSG) derived sensor data.

Name	Type	Data Type	Description	Dimension
SST	input	Byte	CW coded SST (kelvin): 270 + 0.15x<value> (values 0-6 are cloud/land flags)	Grid (0.05°)

While the geostationary data are gridded on the same 0.05° grid as the analysis, the AVHRR SST products are in swath format, *i.e.* original satellite projection. Although there are some 35 layers provided in the ACSPO output SST HDF files, only a few are required by the analysis system. These are shown in Table 3.2.

Table 3.2. Input list of ACSPO polar-orbiting (NOAA-19, METOP) derived sensor data.

Name	Type	Data Type	Description	Dimension
latitude	input	Float	Latitude in degrees	pixel
longitude	input	Float	Longitude in degrees	pixel
acsपो_mask	input	Byte	Combined land/sea/ice/cloud/QC mask	pixel
sst_regression	Input	Float	SST retrieval (kelvin)	pixel

3.2.2 Ancillary Data

The following table lists and briefly describes the ancillary data required to run the analysis.

Table 3.3 Input of ancillary data

Name	Type	Data Type	Description	Dimension
Ice Mask	input	Float	NCEP daily ice concentration	1/12°
RTG_HR SST	input	Float	NCEP daily RTG_HR SST	1/12°

3.2.3 Static and internal analysis/observation state values

In addition to the derived sensor data and the ancillary data, various static and internally updated parameters are read in for each analysis run, such as the land/sea mask (which includes the ocean basins definitions), ocean basins coupling matrix, quad-tree tile overlaps, ocean variability and input SST bias corrections.

3.3 Theoretical Description

The Geo-Polar Blended SST Analysis algorithm is based on work conducted by Khellah *et al.* (2005) and Fieguth (2001). Theoretical details of the algorithm are provided in this section.

3.3.1 Physical Description

The purpose of the analysis is to combine NOAA-generated Level-2 SST products from geostationary and polar-orbiting infrared instruments in an optimal manner. Therefore, underlying physics of SST retrieval behind the derivation of these Level-2 geophysical products is not a primary concern of this ATBD. However, it is worth noting that deficiencies in the retrieval schemes that generate these input products will feed through into the resultant analysis product. In the case of IR-based SST retrievals, these deficiencies are due to various combinations of the following (depending on sensor):

- 1) Instrument calibration error
- 2) Residual cloud contamination
- 3) Inherent non-linearity in the retrieval
- 4) Unmodeled effects (*e.g.* aerosols)
- 5) Surface effects

Instrument calibration error is more of an issue for 3-axis geostationary platforms since the diurnal cycle of instrument heating can be very large (up to 40 kelvin), thus a cycle of order 1 K peak-to-peak is not uncommon simply due to the instrument heating-cooling cycle. Spin-scan geostationary instruments (*i.e.* MSG-SEVIRI) are essentially immune to this particular cycling problem, but may still have other calibration drifts on longer timescales. Polar-orbiting sensors are generally shielded from solar radiation either by the Earth or satellite body for the majority of their orbit, although small calibration glitches may occur as the instrument emerges from Earth shadow. Other aspects of calibration error which apply to all IR sensors to some degree are usually as a result of the pre-launch testing being unrepresentative of the actual on-orbit environment (*e.g.* Mittaz *et al.*, 2009, Mittaz & Harris, 2011). Fixed offsets are often eliminated either inherently in the derivation of algorithm coefficients (*i.e.* when using direct regression of satellite radiance observations against *in situ* data) or by post-validation adjustment of the retrieval algorithm bias term.

Residual cloud contamination usually results in a depressed SST retrieval. However, the need to use the 3.9 micron channel for GOES SST in the daytime means that slight cloud contamination will result in a raised SST retrieval due to the inclusion of extra reflected solar radiation in the observed brightness temperature for that channel.

Inherent non-linearity in the retrieval is due to that fact that, at the time of writing, virtually all SST retrieval algorithms employ an algorithm of the form

$$\text{SST} = a_0 + \mathbf{a}^T \mathbf{y} \quad (3.1)$$

Where \mathbf{a} is a vector of regression coefficients and \mathbf{y} is a vector of channel brightness temperatures. All algorithms of this form essentially rely on the following relation

$$\text{SST} - T_i \propto \text{SST} - T_j \quad (3.2)$$

However, unless second and subsequent channels are identical (and thus yield no additional information), this proportionality relationship will generally only be true for the “mean” retrieval state, while specific retrieval conditions (view angle, water vapor amount, air-sea temperature difference, *etc.*) will dictate the inherent bias due to algorithm non-linearity.

Unmodeled effects such as dust and smoke aerosols will cause biases in SST retrieval since the Level-2 SST algorithms do not generally have sufficient degrees of freedom and/or sensitivity to account for both these and the main atmospheric absorption effects. Dust aerosols are usually generated by aeolian processes in regions of friable material (typically deserts) and may be transported substantial distances in the troposphere. Similarly, smoke aerosol is usually prompted by biomass burning in the dry season. Such events are usually seasonal but may display significant day-to-day variability.

Surface effects are physical processes in the upper ocean which may cause a discrepancy between the radiometric skin temperature (*i.e.* that to which an IR satellite SST is sensitive) and the SST measured at some depth by an *in situ* sensor. The two main processes are the skin effect, due to the conduction of heat flux across a layer of finite thermal diffusivity (typically 0.2 K) and diurnal heating, caused by the buildup of buoyant warm layers of water in times of high insolation and light winds. This latter effect may exceed 6 kelvin in extreme circumstances (Gentemann *et al.*, 2008). Avoidance of this effect is the primary motivation for the nighttime-only product we produce at the request of NOAA CRW (see §2.1).

While it is beyond the remit of this ATBD to suggest improvements to the upstream processing, some attempt must be made to correct the input products prior to the analysis step itself. This is accomplished in the bias correction step, which was previously mentioned in §3.1. Day and night data are treated separately for each sensor in order to mitigate calibration cycle effects, cloud detection differences (cloud detection algorithms are usually different for day and night), different non-linearity effects (generally, different

channel sets are used for day and night retrievals), and differences in surface effects between day and night.

The input product biases themselves need to be assessed with respect to a “bias-free” reference. In this case, the NCEP RTG_HR operational 1/12° analysis is used. Aside from obvious benefit of using an in-house operational NOAA product, the scientific reasons for employing the RTG_HR are sound. Although the RTG_HR does employ AVHRR data, the actual SST observations have been obtained using a physical retrieval methodology, *i.e.*

$$\Delta\text{SST} = \mathbf{G}\delta\mathbf{y} \quad (3.3)$$

where ΔSST is the adjustment to a “first-guess” SST (from the previous day’s RTG_HR analysis), $\delta\mathbf{y}$ is a vector of differences between “first-guess” simulated brightness temperatures and those observed by the instrument, and \mathbf{G} is a gain matrix also calculated from simulation. Since the simulations are performed using local atmospheric profile information, any departure from the linear relation anticipated by Eq. 3.3 is expected to be small. (Note in passing that $\mathbf{G}\delta\mathbf{y}$ implies more than one variable is retrieved since \mathbf{G} is 2-dimensional – usually an adjustment to TPW is also obtained.) Furthermore, the retrievals are additionally bias-corrected with respect to *in situ* data.

3.3.2 Mathematical Description of the Geo-Polar Blended SST Analysis algorithm

Generally, solutions to the problem of analysis of successive time-ordered sequences of SST images (*i.e.* gridded SST observations) fall into the generic prediction-update structure as shown in Fig. 3.1, in which a sequence of observed images $\mathbf{y}(t)$ is processed, predicted estimates of state space $\hat{\mathbf{x}}(t|t-1)$ are predicted from an estimated motion field \mathbf{m}_t , and the

final updated estimates $\hat{x}(t|t)$ are driven by a residual field $v(t)$ which is the information contained in the observations $y(t)$ that was not predicted by $\hat{x}(t|t-1)$.

The solution to this statistical filtering problem is the Kalman filter, whose mathematical structure resembles Figure 3.1:

Prediction Step:

$$\hat{x}(t+1|t) = A\hat{x}(t|t) \tag{3.4}$$

$$\tilde{P}(t+1|t) = A\tilde{P}(t|t)A^T + Q \tag{3.5}$$

Where A is the system dynamics and Q is the process or driving noise.

Update Step:

$$K(t) = \tilde{P}(t|t-1)C(t)^T (C(t)\tilde{P}(t|t-1)C(t)^T + R(t))^{-1} \tag{3.6}$$

$$\hat{x}(t|t) = \hat{x}(t|t-1) + K(t)[y(t) - C(t)\hat{x}(t|t-1)] \tag{3.7}$$

$$\tilde{P}(t|t) = [I - K(t)C(t)]\tilde{P}(t|t-1) \tag{3.8}$$

where measurements $y(t) = C(t)x(t) + v(t)$ with measurement error covariance $R(t)$ are incorporated to improve the estimate of state space with respect to the prediction. Since the dimensions of the matrices are the same as the total number of grid points, it can be

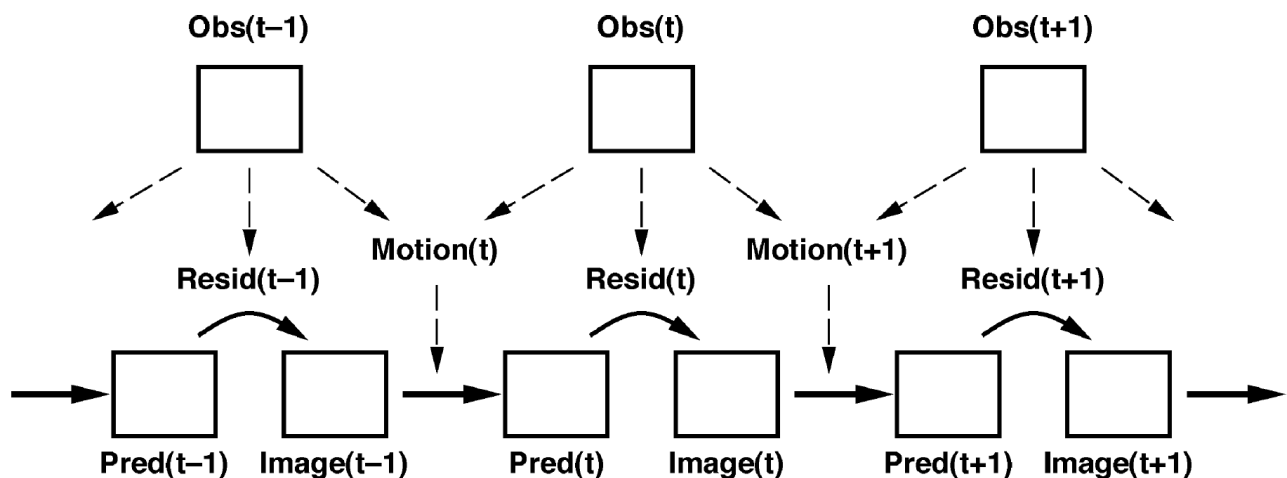


Figure 3.1 Standard prediction-update process. An image sequence can be used to infer motion information and a residual, which determines the time-to-time prediction and update. A wide variety of problems can be cast into this framework. (Taken from Khellah *et al.*, 2005)

seen that a straightforward application of equations 3.4 – 3.8 is completely infeasible for our application. The calculation of the Kalman gain, for example, would require the inversion of a matrix of order 3×10^{14} elements. Also, since the location of cloud-free input data will change for each time period, the statistics become nonstationary and stationarity assumptions cannot be made. Furthermore, any representation for the 2-D covariance $\tilde{P}(t|t)$ must guarantee positive definiteness, and it should also be compatible with the goals of efficient prediction and estimation.

The key to the proposed approach is that the nonstationary prior $\tilde{P}(t+1|t)$ is represented as a spatially-weighted combination of explicit stationary priors which themselves have simple representations, for which positive-definiteness is assured, and are compatible with efficient update methods.

Prediction Step

The 2-D heat diffusion process can be described by

$$\frac{\partial x(i, j, t)}{\partial t} = a \cdot \frac{\partial^2 x(i, j, t)}{\partial i^2} + a \cdot \frac{\partial^2 x(i, j, t)}{\partial j^2} - b \cdot x(i, j, t) + \gamma \cdot w(i, j, t) \quad 3.9$$

where $x(i, j, t)$ represents temperature (or other process of interest) at location (i, j) and time t and $w()$ is unit variance Gaussian white noise. Although ocean dynamics are more complex (nonstationary and nonlinear), the purpose of this model is to develop an estimator based on a model which is sufficient to regularize the space-time interpolation of measurements. The model can be discretized onto an $m \times m$ grid to permit the construction of a system of difference equations

$$\underline{x}(t+1) = A \underline{x}(t) + \underline{w}(t) \quad 3.10$$

Where \underline{x} is a column vector of length $n = m^2$. The dynamics matrix A is penta-diagonal and can be efficiently represented implicitly by a stationary convolution kernel A_k

$$A_k = \begin{bmatrix} 0 & \beta & 0 \\ \beta & \alpha & \beta \\ 0 & \beta & 0 \end{bmatrix} \quad 3.11$$

This allows the exact state prediction to be computed by convolution

$$\hat{\underline{x}}(t+1|t) = A_k * \hat{\underline{x}}(t|t) \quad 3.12$$

However, the prediction of the error statistics is more challenging. In principle, the estimation error may be propagated

$$\tilde{P}(t+1|t) = A\tilde{P}(t|t)A^T + Q \quad 3.13$$

but, as already mentioned, the exact calculation of the full matrix is essentially impossible. The approach for the error prediction step is to parameterize the error covariances. Note that any positive semi-definite matrix P can be written as a product of standard deviations σ and correlation coefficients ρ

$$P = \left\{ \underline{p} \underline{p}^T \right\}^{\frac{1}{2}} \bullet \Phi$$

$$= \begin{bmatrix} \sigma_{(1,1)}^2 & \sigma_{(1,1)}\sigma_{(2,1)} & \cdots & \sigma_{(1,1)}\sigma_{(n,n)} \\ \sigma_{(2,1)}\sigma_{(1,1)} & \sigma_{(2,1)}^2 & & \vdots \\ \vdots & & \ddots & \\ \sigma_{(n,n)}\sigma_{(1,1)} & \cdots & & \sigma_{(n,n)}^2 \end{bmatrix} \bullet \begin{bmatrix} 1 & \rho_{(1,1)(2,1)} & \cdots & \rho_{(1,1)(n,n)} \\ \rho_{(2,1)(1,1)} & 1 & & \vdots \\ \vdots & & \ddots & \\ \rho_{(n,n)(1,1)} & \cdots & & 1 \end{bmatrix} \quad 3.14$$

i.e. P is explicitly expressed in terms of its variances $\underline{p} = \text{diag}(P)$ and its correlation coefficients Φ , where \bullet is element-by-element multiplication. Thus prediction (3.13) may be expressed as

$$\left\{ \tilde{\underline{p}}(t|t)\tilde{\underline{p}}(t|t)^T \right\}^{\frac{1}{2}} \bullet \Phi(t|t)$$

$$\stackrel{\text{Prediction}}{\Rightarrow} \left\{ \tilde{\underline{p}}(t+1|t)\tilde{\underline{p}}(t+1|t)^T \right\}^{\frac{1}{2}} \bullet \Phi(t+1|t) \quad (3.15)$$

The question arises as to how to achieve (3.15), and how to select a positive definite Φ ? The evolution of \underline{p} is at least intuitive since the error variance will decrease near measurements, and increase with every prediction step. However, the form of Φ is much less obvious. It can be shown (Khellah *et al.*, 2005) that neither the Lyapunov nor Riccati solutions are particularly good choices for Φ . However, the issue may be circumvented by modeling Φ in a parameterized form which is known to be positive-definite. The diffusion dynamics model (3.9) implies an exponential correlation structure, and the error structures $\Phi(t|t)$, $\Phi(t+1|t)$ can be modeled

$$\rho(i, j)(i + \tau_i, j + \tau_j) = e^{-\left\{ \frac{|\tau_i| + |\tau_j|}{l(i, j)(i + \tau_i, j + \tau_j)} \right\}} \quad 3.16$$

Where l represents the correlation length. Given (3.16), the problem of how to implement the prediction of (3.15) reduces to the prediction of the diagonal elements of \underline{p} and the correlation lengths $L(t+1|t)$. If we assume that relationships between error variances and correlation lengths may be constructed

$$\begin{aligned} \underline{\tilde{p}}(t|t) &\Rightarrow L(t|t) \\ \underline{\tilde{p}}(t+1|t) &\Rightarrow L(t+1|t) \end{aligned} \quad 3.17$$

It can be shown that, for all stationary exponential cases

$$\frac{\tilde{p}}{p_0} = \frac{\tilde{l}}{l_0} \quad 3.18$$

where p_0 and l_0 are process (Lyapunov) variance and correlation length respectively. Although, for nonstationary problems this linear relationship no longer applies, it remains close to linear for all but small \underline{p} . In general, the relationship may be assumed linear, or inferred experimentally over the range $[l_{\text{small}}, l_{\text{large}}]$ of possible correlation lengths

$$l_{\text{small}} = l_{\text{Riccati}}, \quad l_{\text{large}} = l_{\text{Lyapunov}} \quad (3.19)$$

The propagation of the updated error variances may be expressed

$$\underline{\tilde{p}}(t+1|t) = \text{diag}(A\underline{\tilde{P}}(t|t)A^T + Q) \quad (3.20)$$

Since A is sparse, this product may be performed exactly. The off-diagonal elements of $\underline{P}(t|t)$ that are needed may be computed from the empirical relationship between p and l . Given the updated error variances $p(t|t)$, the correlation lengths $L(t|t)$ are inferred, thus $p(t+1|t)$ and $L(t+1|t)$ may be computed and the predicted error covariance is obtained

$$\hat{P}(t+1|t) = \left\{ \underline{\tilde{p}}(t+1|t) \underline{\tilde{p}}(t+1|t)^T \right\}^{\frac{1}{2}} \bullet \Phi(t+1|t) \quad (3.21)$$

Update Step

Our proposal for overcoming the computationally challenging matrix inversion in (3.6) is to use a multi-scale approach which efficiently solves the update step and produces $p(t|t)$, as needed for prediction. The method has been widely applied in image processing, and models a 2-D field on a quad-tree (see Figure 3.2). Many efficient estimators, including multi-scale, apply to static problems without difficulty. However, the dynamic estimation we require presents a significant challenge. A positive-definite result is only guaranteed for a fixed (*i.e.* stationary) correlation length, not a spatially varying one. The variation in data density precludes easy selection of a single static model – sparse data benefit from a long correlation length that would suppress high-frequency signal in data-dense regions and vice versa. The proposed solution is to perform estimates for a range of stationary correlation lengths and obtaining a weighted combination of the resulting fields.

The two critical factors affecting the computation weights are the number of interpolating priors and the actual choice of correlation lengths. The set of weights may be optimized by minimizing the worst-case fractional error (Khellah *et al.*, 2005)

$$\text{Minimize } \max_l \left(\max_{i,j} \frac{|\hat{x}(i,j,l) - \hat{x}'(i,j,l)|}{\sqrt{\tilde{p}(i,j,l)}} \right) \quad (3.22)$$

The result of this analysis is that, for our problem, a reliable interpolation may be obtained

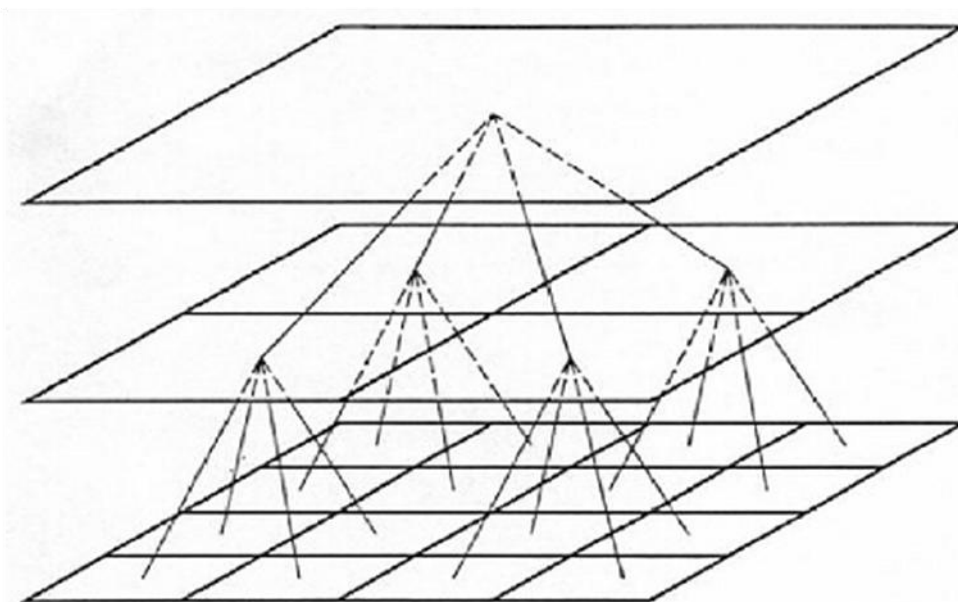


Figure 3.2 Simple multi-scale tree showing the connections between the nodes on three different scales

from three stationary prior models with successive doubling of correlation length.

3.3.3 Summary of Algorithm Selection

The selected algorithm has the benefit of being able to emulate the Kalman filter without the immense (or rather insurmountable) computational burden that a “brute-force” application of the original equation requires. The mimicking of a non-stationary prior model by a combination of stationary priors provides an elegant and robust solution to a long-standing problem. Essentially, the proposed solution should preserve fine-scale detail where it exists in the data, while providing a reasonable estimate of innovation for data-sparse regions.

3.4 Algorithm Output

Output of the Geo-Polar Blended SST Analysis algorithm essentially consists of the analyzed SST for each ocean point on the 0.05 degree grid, the estimated uncertainty and the land/ice/ocean mask data, as shown in Table 3.4.

Table 3.4. Algorithm output data.

Name	Type	Data type	Description
sst_analysis	Output	Float	Analyzed SST for each ocean grid point
error_analysis	Output	Float	Estimate of internal analysis accuracy
mask	Output	Byte	Combined land/ice/ocean basin mask

In addition, the processing will also produce some metadata describing processing information (e.g. date/time stamps), as well as information on the input data that were used in the processing.

Specifically, the common metadata providing general information about the product includes product name, satellites used, projection, product resolution (at nadir), date and time, bounding box, byte order information, product version number, data format/compression type, ancillary data to produce product (including product precedence and interval between datasets is applicable), production location and contact information. Moreover, metadata provides additional statistics on the number of input data points accepted into the analysis step for each platform. Table 3.5 describes the contents of the

NOAA NESDIS STAR

ALGORITHM THEORETICAL BASIS DOCUMENT

Version: 2.0

Date: May 15, 2012

TITLE: Geo-Polar Blended SST Algorithm Theoretical Basis Document

Page 28 of 44

mask data. Since the values are mutually exclusive (with the exception of the ice mask) there is no need for individual bits to be specifically set. As previously mentioned, two analyses are produced at 0.05 degree resolution using satellite observations for day and night, and night-only respectively.

Table 3.5 Detailed descriptions of the mask byte set at the pixel level.

Byte	Bit	Flag	Source	Effect
1	2	Ice	NCEP	0=no ice, 1=ice
	3	Land	UK Met Office	0=ocean, 1=land
	4-6	Ocean basin	STAR	010=Pacific Ocean, 011=Atlantic Ocean, 101=Indian Ocean, 110=Arctic Ocean, 111=Southern Ocean

Note: The ocean basins are essentially an internal device of the analysis to ensure that data from one basin does not erroneously contribute to the analysis field of another if there is no geophysical connection.

3.5 Performance Estimates

3.5.1 Test Data

The performance of the new analysis was evaluated for a period of one month at the end of 2011. Level 2 input SST files were obtained from NESDIS operational processing, while the ancillary NCEP ice concentration and RTG_HR data were obtained from the NESDIS DDS.

3.5.1.1 Geostationary SST Data

Gridded GOES-SST products for the validation period had retrieval accuracies ranging from ~0.6 K (night) to 1.1 K (day) r.m.s., while MTSAT and MSG SST product accuracies for the same period were 0.5-0.6 K (night) and 0.8 K (day) r.m.s.. (See http://www.star.nesdis.noaa.gov/sod/mecb/goes_validation/test/sst_region.php, http://www.star.nesdis.noaa.gov/sod/mecb/mtsat_validation/sst_region.php, and http://www.star.nesdis.noaa.gov/sod/mecb/msg_validation/sst_region.php).

3.5.1.2 Polar-orbiting SST Data

ACSPO AVHRR (NOAA-19 and METOP-A) Level-2 swath SST data products for the validation period had accuracies of 0.4 K (nighttime) and 0.5-0.6 K (day) r.m.s.. (See <http://www.star.nesdis.noaa.gov/sod/sst/squam/ACSPO/index.html#>)

3.5.1.3 Ground Truth Data

The *in situ* data used to validate the analysis originate from the World Meteorological Organization's Global Telecommunications System that broadcast operational data to a variety of users (principally national meteorological services). These data are initially collected by NCEP but then subject to quality control processing via the NESDIS/STAR *in situ* Quality Monitor (iQuam) system (<http://www.star.nesdis.noaa.gov/sod/sst/iquam/>). The data are globally distributed (see Figure 3.3) and number several thousand observations per day. For the purposes of this validation, ship data are excluded and the SST observations for each unique buoy ID are converted to daily averages.

3.5.1.4 Match-ups

To get pairs of valid match-up SSTs from the Geo-Polar Blended SST Analysis and *in situ*

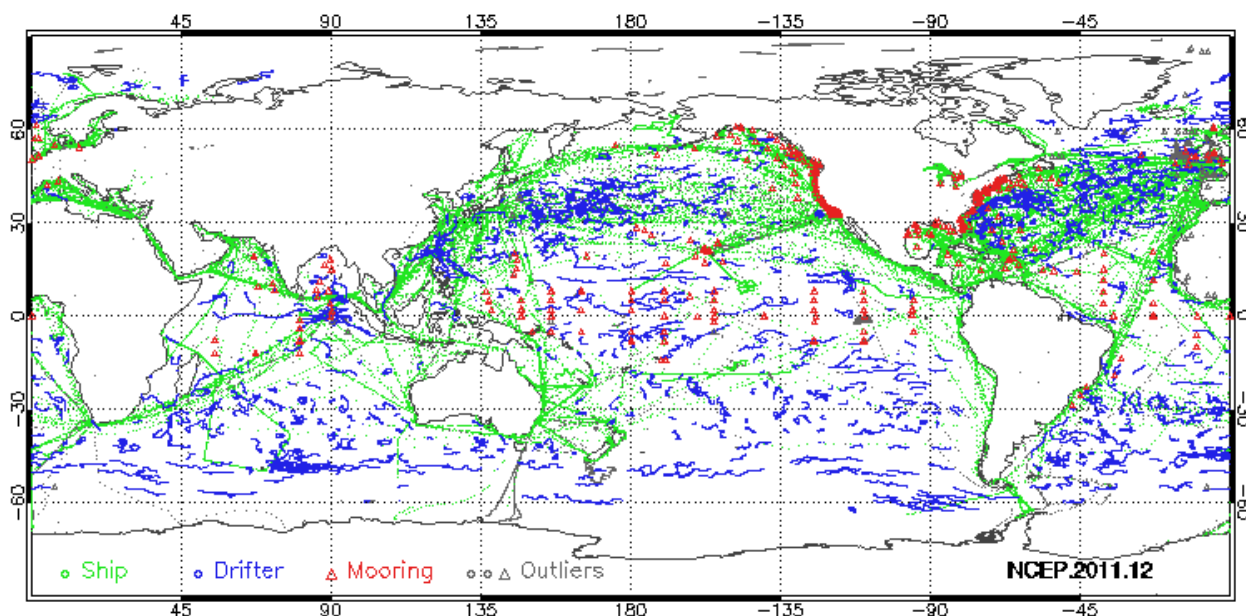


Figure 3.3 Location of *in situ* data from iQUAM database for the validation period. The ship data (green) were not used in the validation

buoy data is essentially straightforward, since the product is global and gap-free. However, some additional quality control was performed in the construction of daily averages for each unique buoy ID:

- 1) There must be at least 5 buoy observations during the 24-hour period
- 2) The standard deviation of the buoy measurements must be no greater than 0.5 K r.m.s..

Finally, some QC is performed with respect to the analysis SST

- 3) All 9 pixels in the 3x3 box centered on the buoy must be valid clear ocean.

3.5.2 Results

The results obtained for the 5 km analysis over the validation period can be seen in Figure 3.4. The robust standard deviation of 0.29 K is slightly better than that obtained for the 11 km analysis over the same time period. It should be noted that the robust standard deviation, derived from median statistics, is a better measure of the main distribution than the simple standard deviation, as illustrated by the green and red Gaussian curves respectively.

Some indication of the possible causes of spread outside the main distribution can be gleaned from studying the results for matches where QC step (2) is changed from 0.5 K to 0.1 K r.m.s.. In the latter case, while the robust standard deviation improves only slightly to 0.28 K, the simple standard deviation improves to 0.35 K (from 0.4 K). Since the QC step in question is essentially independent of the analysis, it may reasonably be concluded that the *in situ* data are the most likely source of outliers.

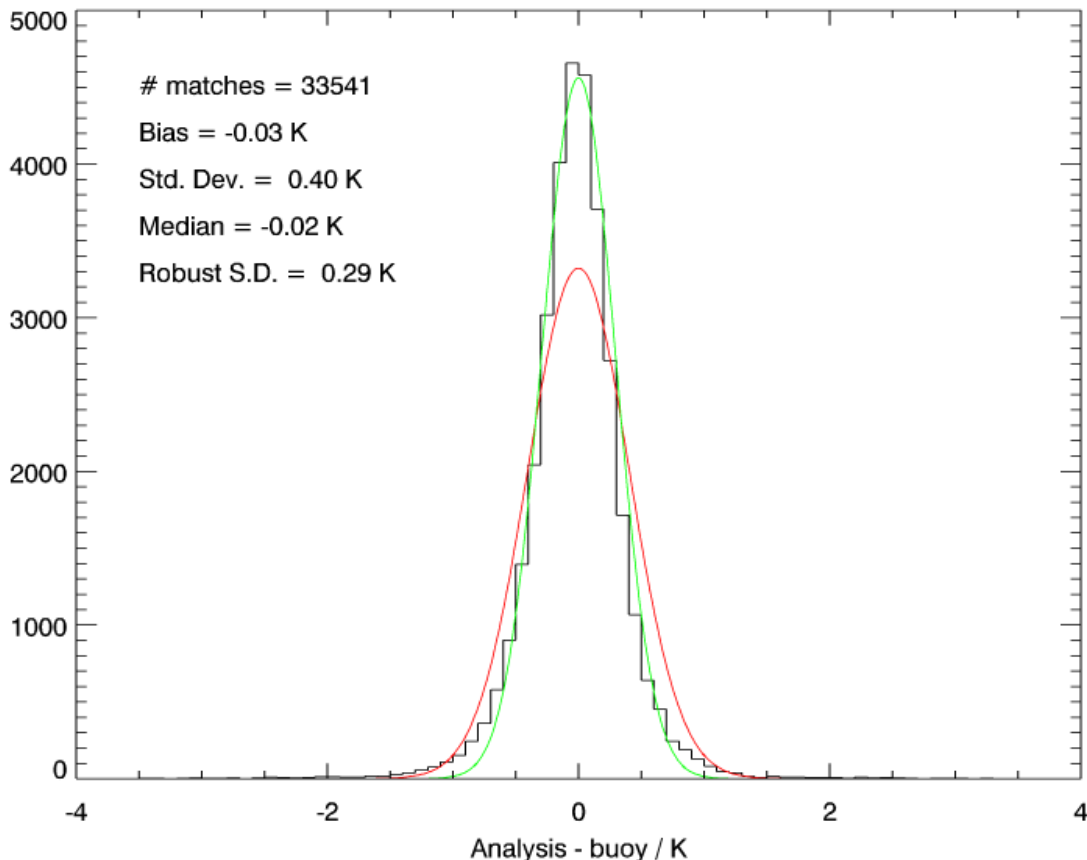


Figure 3.4 Validation of 5-km Geo-Polar Blended SST Analysis against *in situ* buoy data. The robust standard deviation of 0.29 K is the value derived for the green Gaussian curve, which is much more representative of the main peak of the data.

3.5.2.1 Precision and Accuracy Estimates

The validation results shown in the previous section show that the bias (accuracy) over 1 month is -0.03 K, *i.e.* well within the requirement of 0.3 K. The standard deviation of 0.4 K is respectable, and is an improvement on the accuracy of all the input data sources, except perhaps the AVHRR nighttime observations. Since the data are actually dominated by the geostationary observations, which have standard deviations of between 0.5 K and 1.1 K, the analysis can be regarded as a major improvement, especially since it is gap-free. Finally, it should be borne in mind that, unlike many operational analyses, no *in situ* data are used in the analysis. It has been noted (GHRSSST, 2011) that the inclusion of such data inevitably skews the validation results. This is even true when a portion of the data are

withheld during the validation phase (e.g. for the RTG_HR) since bulk SST measurements have a high persistence from day-to-day. Since our analysis is essentially independent of *in situ* data, the accuracies obtained are certainly more realistic than those for other analyses which include such data. Furthermore, the application of robust statistics produces a much better fit to the main peak of validation data and results in a standard deviation of 0.29 K. Such techniques (Merchant and Harris, 1999) are increasingly being employed in the validation of SST data. Validation results for various regions are summarized in Table 3.6.

Table 3.6. Precision and Accuracy (in kelvin)

Region	Bias	Standard Deviation	Robust Standard Deviation
Global	-0.03	0.40	0.29
Northern Extra-Tropics	-0.05	0.47	0.32
Tropics	-0.02	0.35	0.27
Southern Extra-Tropics	-0.03	0.38	0.30

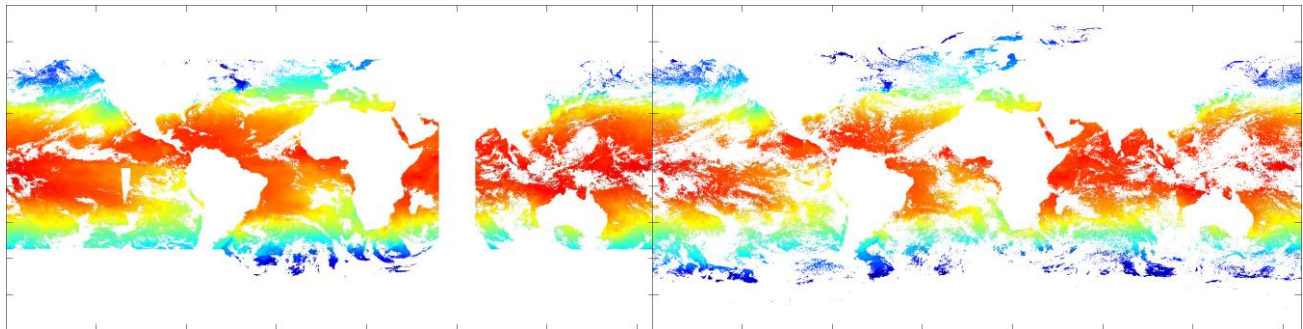


Figure 3.5 One day's worth of geostationary SST data (left panel) and polar-orbiting SST data (right panel). Where the geostationary data are available (the coverage boundaries are reasonably evident) the data density is higher, as evidenced by the fact that regions for which no observation is available are significantly diminished with respect to the polar-orbiting data.

3.5.2.2 Error Budget

The internal analysis error estimates are generally significantly lower (typical value ~ 0.2 K) than those realized in the validation process. However, it should be borne in mind that the *in situ* data used in the validation are themselves subject to error. One study (O'Carroll *et al.*, 2008) estimates the error in drifting buoy data to be 0.23 K which, combined with an internal analysis uncertainty of 0.2 K, means that validation results less than ~ 0.3 K r.m.s. are unlikely to be achieved if the two datasets are independent. Since this is at the same level as the result for the robust standard deviation of the validation data, it might reasonably be concluded that the analysis performs at, or very close to the expected limit. However, while there are no obvious deficiencies, it is worth pointing out that the primary sources of error lie with the input data, *i.e.* the Level-2 satellite SST products. As has already been mentioned, within their coverage region, the geostationary data are generally dominant due to the repeat imaging capability (see Figure 3.5). Furthermore, since their retrieval variances and bias corrections are larger than those for polar-orbiting data, the

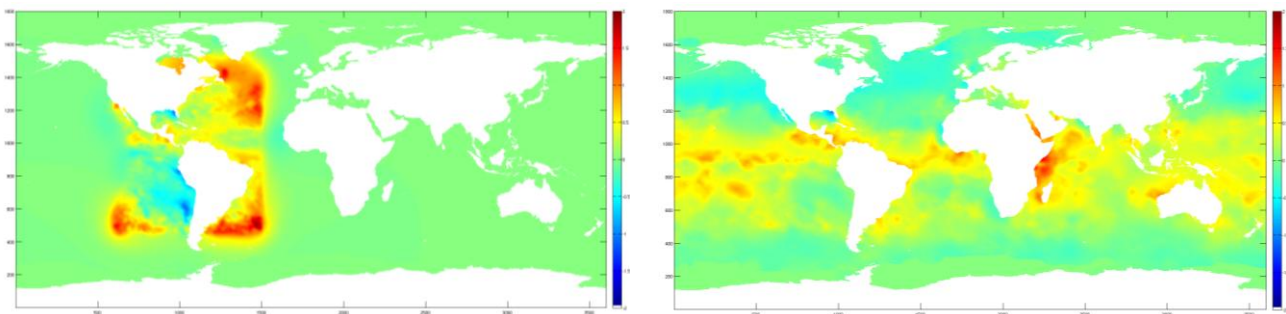


Figure 3.6 Daytime bias correction for GOES-E SST product (left panel) and NOAA AVHRR SST product (right panel). The "saddle point" nature of the bias correction field for the geostationary data is anticipated due to the fixed geometry of the sensor with respect to major atmospheric circulation patterns. The warm biases evident in the AVHRR data for the southern hemisphere are partially due to diurnal warming.

quality of the final analyzed result is most heavily dependent on the ability of the analysis system to account for errors.

Irrespective, the benefits of utilizing geostationary data in the provision of a daily high-resolution (0.05°) SST analysis outweigh the challenges. The primary benefit is, of course, data coverage. Thus the most critical aspect is the effectiveness of the bias correction and the quality control procedures employed during the data ingest phase. Examples of the bias correction fields for GOES SST and AVHRR SST are shown in Figure 3.6. The validation results bear testimony to the success of the analysis system in dealing with the majority of biases in the input data. However, the method is still purely stochastic in nature and improvements could be made by incorporating geophysical information into the prediction of bias for the input data. For example, incorporation of view angle and TPW information may help to account for geophysical sources of bias in the input products.

The error budget of the current processing system may therefore be summarized as a combination of error sources and the success of the bias correction and analysis methodology, as indicated in Table 3.7.

Table 3.7. Error Budget (in kelvin)

Error Source	Random Component	Bias Component	Mitigation %
GOES Daytime SST	~1	≥1	75
GOES Nighttime SST [†]	~0.6	~1	75
MTSAT Daytime SST	~0.8	0.7	70
MSG Daytime SST	~0.8	~0.5	70
MSG Nighttime SST [†]	~0.6	~0.5	70
AVHRR Daytime SST	~0.5	~0.5	60
MTSAT Nighttime SST [†]	0.5	0.5	70
AVHRR Nighttime SST [†]	~0.4	~0.4	60
RTG_HR SST [†]	0.4	≤0.5*	0

*the RTG_HR SST is usually biased by ~0.1 K but can occasionally drift

[†]these data are also used as inputs to the nighttime-only 5-km analysis product

3.6 Practical Considerations

The analysis is implemented on a single compute server, rather than a supercomputer. Thus, there are significant requirements with respect to computational efficiency. The high-resolution nature of the 0.05° analysis means that a 64-bit system is required, with at least 16 GB of main memory, in order to hold all of the gridded input data types at full model resolution and double-precision. The computing efficiencies have already been mentioned in §3.3.2 but specific information is provided in the next section.

3.6.1 Numerical Computation Considerations

The use of a quad-tree structure implies a fundamental base unit which is subject to the quad-tree “divide-and-conquer” process. This base unit or ‘tile’ therefore needs to be square with dimensions that are a power of 2. The number of levels of the quad-tree is therefore dictated by the power of 2 that is chosen to define the tile size. Tiles are processed independently but will inevitably overlap to some extent, unless the domain dimensions themselves are powers of 2. In order to avoid artifacts at tile boundaries, it is sensible to ensure overlap between the tiles that is of the order of the longest correlation length (in grid cell units) that will be employed in the analysis. The three correlation lengths that are used are 8, 16 and 32 pixels, thus an overlap of at least 32 pixels between each tile is desirable. Fixed offsets and overlaps in X and Y must be defined that ensure adequate overlap and exact coverage of the full domain. Generally, while adequate overlap is desired, excessive overlap will result in many more tiles being processed than is necessary to achieve a satisfactory outcome, since the greater the overlap, the smaller the fractional domain coverage per tile (see Figure 3.7). Table 3.8 shows the quantities that need to be specified, along with their values.

Table 3.8. Quad-tree tile parameters

Parameter	Derivation	Value
Number of quad-tree levels (sc)	–	8
Tile size (sizc, sizr)	2^{sc-1}	128
Column (X) overlap (oc)	$(sizc-oc) \text{ MOD } 7200 = 0$	56
Column offset (ofsc)	$-(oc/2 - 1)$	-27
Row (Y) overlap (or)	$(sizr-or) \text{ MOD } (3600-sizr) = 0$	66
Number of tile columns (numc)	$7200 \div (sizc-oc)$	100
Number of tile rows (numr)	$(3600-sizr) \div (sizr-or) + 1$	57



Figure 3.7 Relationship between full domain and individual tiles. The full domain (7200x3600 pixels) is represented by the large rectangle, while the tiles are light blue squares. Where tiles overlap the blue shading is darker. The full size of a tile is illustrated by the red square, while the purple shaded area represents the effective domain coverage of the tile.

3.6.2 Programming and Procedural Considerations

The analysis system is run under Matlab. Data are preprocessed using Matlab routines and passed to the multi-scale analysis routine. The analysis code itself is written in C and compiled using the Matlab 'mex' function, which allows C subroutines to be called directly from Matlab as if they were native Matlab functions. While the routines have already been compiled to run under Red Hat Linux, there are compile scripts which have been made available to ensure that the code can be ported to another system with an appropriate Matlab license. Recent experience has shown that some care must be taken to ensure that the `gcc` libraries available on the system must be compatible with those expected by the Matlab 'mex' utility. Generally, incompatible libraries will be signaled at link time.

3.6.2.1 Configuration of Analysis System

The analysis system itself is currently configured using two files which specify key information. The `init_par_info.m` file specifies information related to directory structures, generic and specific file names, e.g. location of Matlab routines, raw and preprocessed satellite SST directories, and the name of the land mask file to use. The `init_par_info.m` file specifies parameters related to the analysis processing, such as

resolution, domain size, quality control thresholds to employ for each data type and correlation lengths.

The analysis system itself can be controlled directly from the Matlab command line. However, for routine processing, a `bash` control script, `mkbledned_5km.sh`, is used to execute the program. The script offers the option to run the analysis with all, partial or no raw data ingestion, as well as running only the preprocessing steps for various input data types.

All the code (Matlab, C and `bash`) is under configuration control in a `cvcs` repository on the OSPO server.

3.6.3 Quality Assessment and Diagnostics

The product includes an estimate of analysis uncertainty for each pixel. As already mentioned in §3.5.2.4, this is a measure of the internal analysis uncertainty rather than total error, and is therefore only strictly applicable if the input data are without bias (or at least the bias correction is successful) and the residual signal is noise-limited. The processing generates a detailed log file, including the statistics for data rejection/absence, and this also serves as a useful guide to product fidelity for a particular run. The data are continuously validated against *in situ* data and compared to the Reynolds $\frac{1}{4}^{\circ}$ Daily OI SST product (see http://www.star.nesdis.noaa.gov/sod/mecb/blended_validation/sst_monitor.php), where difference maps are produced. The product may also be compared to many other analysis and sources of *in situ* data via the SQUAM verification utility (previously referenced in §3.5.1.2).

3.6.4 Exception Handling

There are two main types of exception that may occur during the processing, each relating to unavailability of data. For geostationary data, expected file sizes are fixed and if the last part of a file is missing then the absent pixels are ignored and processing is still performed on the valid pixels. For the polar-orbiting data, the HDF reading routines intrinsically handle partial files in a similar manner. Neither of the above conditions is deemed sufficient cause for the analysis to abort. The case is similar for input files that are wholly absent. Even if no satellite data are available, the analysis will still run with the thinned RTG_HR SST as it's only input (the result will essentially possess many of the same qualities as the RTG_HR, *i.e.* smoother SST features).

The exceptions which are regarded as critical concern the availability of the ancillary data from NCEP, *i.e.* the daily ice mask and the RTG_HR SST products. Absence of either of

these will cause the analysis to terminate execution with a warning written to the log file identifying the problem.

3.7 Validation

Validation has already been described quite extensively in §3.5. As already described in §3.6.3, the analysis is continuously validated against *in situ* data and compared to the Reynolds $\frac{1}{4}^\circ$ Daily OI SST product .

4. ASSUMPTIONS AND LIMITATIONS

4.1 Assumptions

The primary assumption of the algorithm is that the data are (or can be rendered) bias-free prior to the analysis step. As evidenced by Figure 3.6, bias correction of the input data is critical, since the discrepancies may be large (certainly in excess of 1 K). The current bias correction scheme assumes that, for each data type, the biases are reasonably static over the period of one day. While this may generally be true for clear-air effects (algorithm-related SST retrieval errors), errors due to residual cloud are unlikely to be static. In the latter regard, it is therefore assumed that individual cloud contaminated pixels will either be filtered out by quality control in the gridding step or, if the contamination is 'mild', their impact is diminished by the inclusion of good data (e.g. from other geostationary images) within the same grid cell.

Another critical assumption is that the bias correction reference, the RTG_HR SST, is itself bias-free. While the reasons for expecting this to be the case have already been outlined in §3.3.1, it has been noted that the biases in the Geo-Polar Blended SST analysis closely track those observed in the RTG_HR SST product (e.g. see <http://www.star.nesdis.noaa.gov/sod/sst/squam/L4/index.html#>).

4.2 Limitations

The most important limitation of the algorithm is the need for an external bias correction reference. This precludes it from generating a truly independent climate-quality SST analysis. Another key aspect is that, in the absence of input data, feature resolution is lost over time. In essence, because the model has no predictive skill in the absence of observations, structures are not preserved. The model is therefore reliant on the availability of high-resolution (at least ~5-km) satellite data, which implies IR sensors for the foreseeable future.

4.3 Potential Improvements

There are a number of improvements that have been identified and requested by users, and a project has been initiated under the STAR Enterprise Product Lifecycle process in order to implement the desired changes.

4.3.1 Improved Validation Methods

As has already been alluded to in §3.5.2.3, the use of *in situ* data with accuracy of ~0.2 K represents a limit to the achievable standard of verification. While the Geo-Polar Blended SST Analysis does not explicitly include *in situ* data, the RTG_HR does. It should be noted, however, that, in the presence of satellite data (*i.e.* the majority of the ocean on any

given day, as evidenced by Figure 3.5) the [thinned] included RTG_HR data are completely overwhelmed by observations, perhaps by as much as 100:1 or more. Nevertheless, validation against more accurate, independent *in situ* data would benefit the analysis, the former aspect being more important than the latter in this case. There has been ongoing discussion between the Data Buoy Cooperation Panel and GHRSSST about more accurate drifters, as well as the utility of Argo near-surface measurements for validation.

4.3.2 Algorithm Improvement

Since the major source of error is generally recognized to be the input SST data, we anticipate improvements in analysis quality as the Level 2 products themselves are improved. Physical retrieval methodology is being implemented for the NOAA Geo-SST processing, which promises reduced bias and scatter *cf.* the current operational products. Similarly, ongoing improvements in cloud detection will inevitably benefit the product. The inclusion of full-resolution (1-km) AVHRR data from METOP (the so-called FRAC product) should not only improve the noise statistics via more data averaging, but also permit more sophisticated screening of individual input pixels, since it will be possible to build up a more reliable estimate of population variance and thereby improve outlier rejection.

The analysis may further be improved by utilizing a better bias correction reference. As has already been mentioned, the analysis is currently tied to the quality of the RTG_HR product. The inclusion of additional data (*e.g.* from a more accurate satellite instrument) may help in this regard. Part of the plan for upgrading the system was to include data from the highly accurate Advanced Along-Track Scanning Radiometer. However, the recent problems with the ENVISAT platform may necessitate development of an alternative strategy.

While the inclusion of geostationary data results in high resolution analyzed SST fields for many locations, regions of persistent cloud cover are only forced by the thinned RTG_HR data. Since the RTG_HR analysis itself only uses AVHRR as input (and the *in situ* data), the resultant analysis resolution is rather poor. The proposed solution is to incorporate SST observations from microwave instruments. The original plan envisaged the use of AMSR-E data, but the sensor failed in October 2011. Although WindSat data could be used, the desire for an operational data stream means that the current intent is to incorporate SSTs from the AMSR-2 instrument which is due for launch on the Japanese GCOM-W1 satellite in May, 2012. AMSR-2 data will be processed in-house at NOAA. Although the native resolution of microwave SST data is much coarser than 0.05° , it should still result in a significant improvement in the analysis for regions of persistent cloud.

Finally, since all satellite observations are potentially subject to the phenomenon of diurnal heating (mentioned in §3.3.1), there are plans to incorporate a diurnal adjustment to the

NOAA NESDIS STAR

ALGORITHM THEORETICAL BASIS DOCUMENT

Version: 2.0

Date: May 15, 2012

TITLE: Geo-Polar Blended SST Algorithm Theoretical Basis Document

Page 42 of 44

input data as part of the preprocessing. One important aspect of this is that it will be necessary to provide a reliable estimate of the uncertainty in the predicted diurnal warming in order to properly weight satellite observations which have the correction applied. The nighttime-only 5-km SST product that we generate using only the nighttime level-2 SST products as input to the analysis is an alternative means of avoiding such diurnal heating effects, although this means that half of the satellite data are not used.

5. LIST OF REFERENCES

- Fieguth, P.W. et al., Mapping Mediterranean altimeter data with a multiresolution optimal interpolation algorithm, *J. Atmos. Ocean Tech*, 15 (2): 535-546, 1998.
- Fieguth, P., Multiply-Rooted Multiscale Models for Large-Scale Estimation, *IEEE Image Processing*, 10 (11), 1676-1686, 2001
- Gentemann, C.L., P.J. Minnett, P. LeBorgne, and C.J. Merchant, Multi-satellite measurements of large diurnal warming events, *Geophysical Research Letters*, 35, L22602, 2008.
- GHR SST, The Proceedings of the XII GHR SST Science Team Meeting, Edinburgh, June 27 – July 1, 2011. GHR SST Project Office, 2011.
- Khellah, F., P.W. Fieguth, M.J. Murray and M.R. Allen, Statistical Processing of Large Image Sequences', *IEEE Transactions on geoscience and remote sensing*, 14 (1), 80-93, 2005
- Maturi, E., A. Harris, C. Merchant, J. Mittaz, B. Potash, W. Meng and J. Sapper, NOAA'S Geostationary Operational Environmental Satellites - Sea Surface Temperature (GOES-SST) Products, *Bull. Am. Meteorol. Soc.*, **89**, 1877-1888, 2008
- Merchant, C.J. and A.R. Harris, On the elimination of bias in satellite retrievals of skin sea surface temperature - II: comparison with in situ measurements, *J. Geophys. Res.*, 104, 23,579-23,590, 1999.
- Mittaz, J.P.D., A.R. Harris and J.T. Sullivan, A Physical Method for the Calibration of the AVHRR/3 Thermal IR Channels 1: The Prelaunch Calibration Data, *Journal of Atmospheric and Oceanic Technology*, 26(5), 996-1019, 2009.
- Mittaz, J.P.D. and A.R. Harris, A Physical Method for the Calibration of the AVHRR/3 Thermal IR Channels 2: An In-Orbit Comparison of the AVHRR Longwave Thermal IR Channels on board MetOp-A with IASI, *Journal of Atmospheric and Oceanic Technology*, 28(9), 1072-1087, 2011.
- O'Carroll, A.G., J.R. Eyre, and R.W. Saunders, Three-Way Error Analysis between AATSR, AMSR-E, and In Situ Sea Surface Temperature Observations, *Journal of Atmospheric and Oceanic Technology*, 25(7), 1197-1207, 2008.

NOAA NESDIS STAR

ALGORITHM THEORETICAL BASIS DOCUMENT

Version: 2.0

Date: May 15, 2012

TITLE: Geo-Polar Blended SST Algorithm Theoretical Basis Document

Page 44 of 44

Reynolds, R.W., and T.M. Smith, Improved Global Sea Surface Temperature Analyses Using Optimum Interpolation, *Journal of Climate*, 7(6), 929-948, 1994.

END OF DOCUMENT